

Numerical simulation of vacuum-ultraviolet irradiation of dielectric layers

H. Sinha,¹ H. Ren,¹ A. Sehgal,¹ G. A. Antonelli,² Y. Nishi,³ and J. L. Shohet^{1,a)}

¹*Department of Electrical and Computer Engineering and Plasma Processing Technology Laboratory, University of Wisconsin–Madison, Madison, Wisconsin 53706, USA*

²*Novellus Systems, Tualatin, Oregon 97062, USA*

³*Stanford University, Stanford, California 94305, USA*

(Received 9 February 2010; accepted 15 March 2010; published online 8 April 2010)

Vacuum-ultraviolet irradiation produces trapped charges in dielectrics. The trapped charges often generate self-consistent electric fields. A Monte Carlo simulation coupled with a Poisson equation solver is used to model the relationship between the irradiation photon flux and electrostatic potential. The simulation includes photoconduction, photoemission, photoinjection, and the effects of self-consistent electric fields. Calculations show that photoemission and photoinjection are responsible for changes in the electric potential as photon dose or dielectric thicknesses are varied. Experimental surface-potential measurements were made to compare the results of the simulation. © 2010 American Institute of Physics. [doi:10.1063/1.3386531]

In processing of microelectronic devices, dielectrics are often exposed to plasmas from which vacuum ultraviolet (VUV) irradiation takes place. The VUV initiates photoabsorption, photoconduction, photoemission, and photoinjection.¹ These processes produce trapped charges in the dielectric,^{2,3} that can adversely affect the electrical properties of the dielectric,⁴ and often produce self-consistent electric fields.⁵ In this work, we utilize a Monte Carlo simulation to model the above four processes. We include charged-particle dynamics with the addition of self-consistent electric fields calculated with a particle-in-cell Poisson algorithm.^{6,7} We calculate the potential in silicon nitride (SiN) deposited on Si and compare it with experimental measurements.

We begin with VUV photons penetrating into the dielectric. Depending on the photon mean free path and the dielectric thickness, photon absorption takes place either in the dielectric or the underlying substrate.⁸ The photon mean free path is a function of the photon energy and the dielectric.⁹ To calculate the mean free path, linear attenuation cross-sections from the National Institute of Standards and Technology were used.⁹

Photon absorption can result in electron-hole-pair production.¹⁰ Here, the additional photon energy not used in pair production is assumed to be kinetic energy of the electrons. Comparing silicon (Si) and SiN, the generated electrons in SiN gain less kinetic energy because the band gap of SiN is larger than the band gap of Si. We neglect the effect of holes on photoconduction, because hole mobility is small compared with electron mobility.¹¹

During photoconduction, electrons undergo displacement and scattering.⁴ To model displacement, the mean free path between successive scatterings was calculated using Mott cross section and dielectric/substrate densities.¹² To model the change in electron trajectories, both isotropic and Rutherford scattering are included.¹³ The scattering angles were determined with elastic-scattering cross sections. To compensate for the energy loss during scatter-

ing, the continuous-slowning-down approximation was implemented.¹⁴

During photoconduction, electrons can be photoemitted from the dielectric. For photoemission, the electron energy at the dielectric-vacuum interface must be greater than the electron affinity of the dielectric.^{15,16} If an electron is to be photoemitted, it should have this energy when it reaches the dielectric-vacuum interface even after multiple scatterings. Electron photoemission leads to generation of trapped positive charges in the dielectric.^{5,15,16} Since electrons near the dielectric-vacuum interface are more likely to be photoemitted, the accumulation of trapped positive charge is expected to be in this region.

It is also possible for electrons to be photoinjected across the dielectric-substrate interface. For photoinjection to occur the electron energy must be greater than the dielectric-substrate interface-barrier energy.^{15,16} Photoinjection can occur from the substrate or *vice-versa*. However for SiN–Si, more electrons are expected to be photoinjected into SiN because electrons in Si have higher energies upon generation. The photoinjected electrons undergo photoconduction and may recombine with trapped positive charges.¹⁶ Thus, photoinjection of electrons reduces the amount of trapped positive charge. Since the substrate is grounded, the holes in the substrate recombine with electrons from ground, preserving charge neutrality.

Thus, the processes of photoconduction, photoemission, and photoinjection create a charge distribution that generates local self-consistent electric fields. Some of the field lines start below the interface and terminate at the substrate ground while others cross the dielectric-vacuum interface into the vacuum. The self-consistent electric field causes drift motion of the electrons and holes.¹¹ This affects the dielectric as follows.

The electric field from the dielectric into the vacuum reduces photoemission, as the electrons have to overcome electrostatic potential. In addition, the electric field directed from the dielectric into the substrate enhances the photoinjection of electrons into the dielectric. Finally, the electrostatic fields enhance the conduction of electrons toward the trapped positive charges. These three effects reduce the number of trapped charges contained in the dielectric. To include

^{a)}Electronic mail: shohet@engr.wisc.edu.

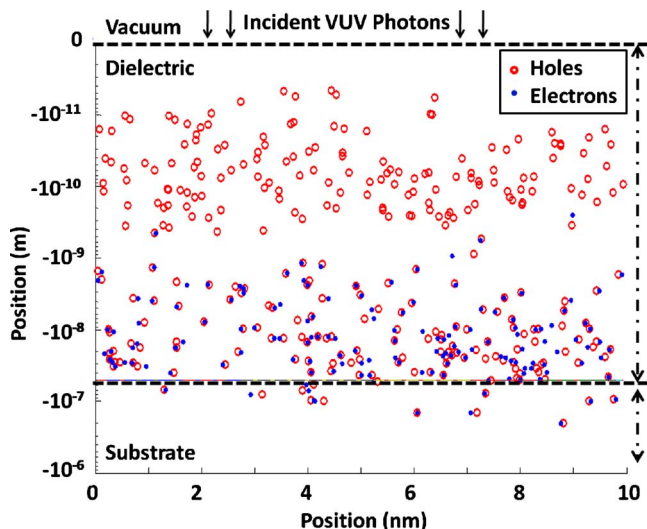


FIG. 1. (Color online) Electron and hole distributions in SiN-Si after irradiation with 20 eV photons at a dose of 5.6×10^{12} photons/cm². The position scale is logarithmic.

these effects, the simulation must calculate the self-consistent electric fields.

These fields are found using a particle-in-cell algorithm to solve Poisson's equation.^{6,7} As shown in Fig. 1, the boundary conditions for the electrostatic potential are as follows. (1) The backside of the substrate is grounded. (2) The potentials on the vertical sides of the simulation were assumed to be equal at each point and were, thus made periodic. (3) At a distance of 1 cm above the dielectric-vacuum interface, the potential is assumed to be zero. Photoemitted electrons were reinjected into the substrate at the grounded back side. Using a sparse-matrix algorithm, the electrostatic potential at each mesh point was obtained by successive relaxation.

Three dielectric thicknesses (50, 250, and 450 nm) of SiN on the Si substrate were examined. The simulation shows that for 20 eV photons the maximum accumulation of trapped positive charges occurred within ~ 4 nm of the dielectric vacuum interface for all thicknesses. Figure 1 shows the distribution of electron and holes in 50 nm thick SiN after it was irradiated with a dose of 5.6×10^{13} photons/cm².

To examine the electrostatic potential as a function of photon dose, we simulate 20 eV photon irradiation on a 250 nm thick SiN sample as shown in Fig. 2. The calculations show that the potential increases from zero to a maximum at the dielectric-vacuum interface as shown in Fig. 2(a). By examining the potential gradient, it is seen that the electric fields are highest in the dielectric. Figure 2(b) shows the potential with a finer scale near the dielectric vacuum interface. It is seen that the electric field reverses at a depth of 2 nm. This is because, as seen in Fig. 1, the net positive charge in the dielectric is highest at this location.

From the potential data, we calculated a surface potential (dielectric-vacuum interface potential) of 1.8 V after a photon dose of 2.3×10^{14} photons/cm². The electric field in the dielectric was calculated to be 3.2×10^6 V/m directed from the dielectric-vacuum interface toward the substrate. A much lower electric field of 3.9×10^3 V/m was calculated in the substrate. With increasing photon dose, the electrostatic potential increases everywhere. The surface potential increased to 3.1 V after the dose was doubled to 4.6

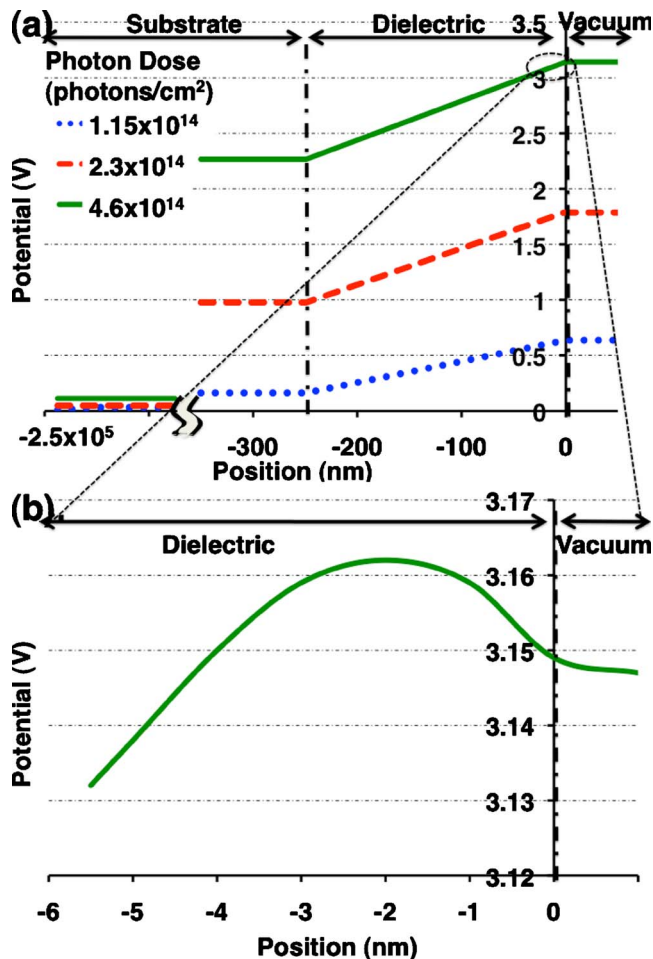


FIG. 2. (Color online) Electrostatic potential as a function of depth in a 250 nm thick SiN dielectric layer with an underlying Si substrate as a function of dose of 20 eV photons. (a) potential distribution from substrate to vacuum (b) potential distribution near the dielectric-vacuum interface.

$\times 10^{14}$ photons/cm². The electric field in the dielectric increased slightly to 3.5×10^6 V/m.

The simulation shows that the electrostatic potential in a sample after VUV irradiation depends on the dielectric thickness. Figure 3 shows the computed surface-potential variation in the three test samples as a function of photon dose.

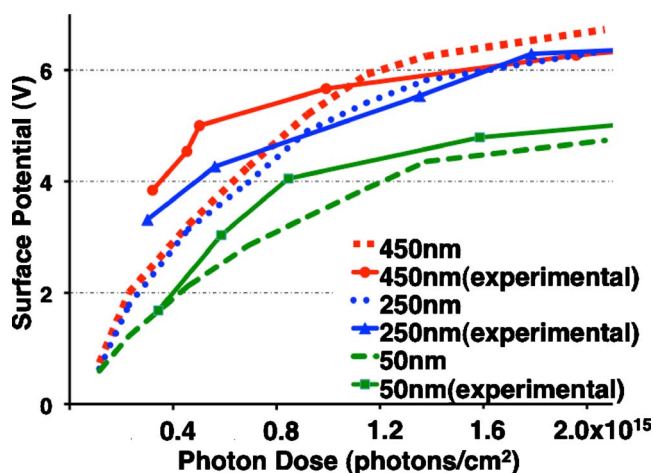


FIG. 3. (Color online) Surface-potential calculations for 50, 250, and 450 nm thick SiN as a function of dose of 20 eV photons compared with experimental measurements.

We observe that thicker dielectrics generate higher surface potentials for the same dose. However, the calculations showed that there was no appreciable change in photoemission with varying thickness. The photoemission current decreases and saturates with increasing photon dose. At the same time, we find that the photoinjection current increases and saturates with photon dose until it equals the photoemission current.¹

Thus, we conclude that the increase in surface potential with thickness is due to the decrease in photoinjected electrons from the substrate into the dielectric, since with increasing thickness, fewer photons reach the substrate. In addition, after a dose of 2.3×10^{14} photons/cm², for 250 nm thick SiN, the electric field in the dielectric was 3.2×10^6 V/m compared to 3.44×10^6 V/m for 50 nm thick SiN. This indicates that the combination of fewer electrons available for photoinjection and the concomitant reduction in photoinjection and photoconduction due to the lower electric field results in more trapped positive charges and higher surface potentials in thicker dielectrics.

For experimental correlation, SiN of thicknesses 50, 250, and 450 nm were deposited on a Si by plasma enhanced chemical vapor deposition (PECVD). These samples were irradiated with 20 eV photons at the Synchrotron Radiation Center (UW-Madison). Surface-potential measurements were obtained with a Kelvin probe and are shown in Fig. 3. Since the dielectrics exhibit a small residual surface potential before VUV exposure, it is difficult to compare the simulation results for low photon fluxes. Nevertheless, there is good agreement with the simulation.

Based on these results, we believe that Monte Carlo simulation coupled to a Poisson solver provides an effective modeling technique that can be used to determine the rela-

tionship between photon flux and energy and the resulting potentials in dielectrics.

This work was supported by the Semiconductor Research Corporation under Contract No. 2008-KJ-1781. The UW Synchrotron is supported by NSF Grant No. DMR-0084402.

¹G. S. Upadhyaya, J. L. Shohet, and J. L. Lauer, *Appl. Phys. Lett.* **86**, 102101 (2005).

²B. Jinnai, T. Nozawa, and S. Samukawa, *J. Vac. Sci. Technol. B* **26**, 1926 (2008).

³H. C. Shin and C. Hu, *Semicond. Sci. Technol.* **11**, 463 (1996).

⁴C. T. Gabriel and J. P. McVittie, *Solid State Technol.* **35**, 81 (1992).

⁵J. L. Lauer, J. L. Shohet, and R. W. Hansen, *J. Vac. Sci. Technol. A* **21**, 1253 (2003).

⁶W. H. Press, S. A. Teukolsky, W. T. Vetterling, and B. P. Flannery, *Numerical Recipes: The Art of Scientific Computing* (Cambridge University Press, Cambridge, 1986).

⁷R. W. Hockney and J. W. Eastwood, *Computer Simulation Using Particles* (McGraw-Hill, New York, 1981).

⁸S. M. Seltzer, *Monte Carlo Transport of Electrons and Photons* (Plenum, New York, 1988).

⁹C. T. Chantler, K. Olsen, R. A. Dragoset, A. R. Kishore, S. A. Kotochigova, and D. S. Zucker, *X-Ray Form Factor, Attenuation and Scattering Tables* [Online] Available: <http://physics.nist.gov/ffast> [2009, December 29]. National Institute of Standards and Technology, Gaithersburg, MD.

¹⁰L. R. Canfield, J. Kerner, and R. Korde, *Appl. Opt.* **28**, 3940 (1989).

¹¹R. S. Muller and T. I. Kamins, *Device Electronics for Integrated Circuits* (Wiley, New York, 2003).

¹²Z. Czyżewski, D. MacCallium, A. Romig, and D. C. Joy, *J. Appl. Phys.* **68**, 3066 (1990).

¹³L. Reimer and B. Lodding, *Scanning* **6**, 128 (1984).

¹⁴R. Shimizu and Z.-J. Ding, *Rep. Prog. Phys.* **55**, 487 (1992).

¹⁵H. Sinha, J. L. Lauer, M. T. Nichols, G. A. Antonelli, Y. Nishi, and J. L. Shohet, *Appl. Phys. Lett.* **96**, 052901 (2010).

¹⁶J. L. Lauer, G. A. Antonelli, Y. Nishi, and J. L. Shohet, personal communication (July 2009).